Single-Molecule Experiments in Vitro and in Silico
Marcos Sotomayor, *et al.*
Science **316**, 1144 (2007);
DOI: 10.1126/science.1137591

REVIEW

Single-Molecule Experiments in Vitro and in Silico

Marcos Sotomayor and Klaus Schulten*

Single-molecule force experiments in vitro enable the characterization of the mechanical response of biological matter at the nanometer scale. However, they do not reveal the molecular mechanisms underlying mechanical function. These can only be readily studied through molecular dynamics simulations of atomic structural models: "in silico" (by computer analysis) single-molecule experiments. Steered molecular dynamics simulations, in which external forces are used to explore the response and function of macromolecules, have become a powerful tool complementing and guiding in vitro single-molecule experiments. The insights provided by in silico experiments are illustrated here through a review of recent research in three areas of protein mechanics: elasticity of the muscle protein titin and the extracellular matrix protein fibronectin; linker-mediated elasticity of the cytoskeleton protein spectrin; and elasticity of ankyrin repeats, a protein module found ubiquitously in cells but with an as-yet unclear function.

Modelers, carrying out molecular dynamics (MD) simulations (*1*), are not content anymore to merely describe biomolecules in a hands-off manner. Rather, they move from pure description to investigative manipulation, seeking knowledge from poking with Nature's biomolecules in so-called steered molecular dynamics (SMD) (*2*) simulations. Modelers got the idea from single-molecule force spectroscopy, which stretches proteins and DNA in manifold ways in vitro (*3*–*5*), but also from the living cell itself, which makes its molecules endure manifold forces in vivo as a result of countless mechanical processes, from control of the unwieldy genome to motor-driven transport (*6*, *7*). The modelers reenact "in silico" (through computer modeling) what atomic force microscopy (AFM), optical tweezer experiments, or the cell do to biomolecules, but they also devise their own "experiments," ones that are as-yet impossible to do in the laboratory.

In silico single-molecule force spectroscopy grew up fast: Nurtured first with ideas from experiments, modelers quickly became partners in the laboratory, explaining old and suggesting new experiments and now even moving ahead of in vitro work. Yet conventional experimentalists observe the real world, whereas computational experimentalists observe only the virtual world of simulation. Can their message be trusted? Clearly there is no general answer, but successes suggest that computational experiments reveal valuable new information on the molecular mechanisms underlying cellular mechanics. We review discoveries made through in silico experiments on the muscle protein titin (*8*–*10*), the closely related extracellular matrix protein fibronectin (*11*), the cytoskeleton protein spectrin (*12*, *13*), and the repeat protein ankyrin (*14*). Appreciation for the value of in silico experiments may be best evidenced by the fact that single-molecule spectroscopists have started to do simulations (*15*, *16*)

Molecular dynamics simulations that mechanically manipulate proteins (*17*, *18*) were initiated a decade ago in response to one of the first AFM experiments on biomolecules by Gaub *et al*. (*19*). The experiments made use of reagents widely used in the laboratory as gluing biomaterials, avidin and biotin. The tetrameric protein avidin binds biotin in its four pockets; biotinylating substrates A and B and adding avidin can bond A and B together. Biotinylating an AFM tip and a substrate permitted Gaub *et al*. to measure, as a function of distance, the forces experienced in making and breaking the biotin-avidin bond. Distance-force curves obtained by Grubmüller *et al*. (*20*) and by Schulten *et al*. (*21*) in SMD simulations revealed that avidin not only has a strong affinity for biotin when completely bound but also follows an unbinding pathway characterized by a series of interactions between biotin and avidin's amino acid side groups. Evans and Ritchie (*22*) used the data from simulation (*21*) to construct the energetics of biotin binding in good agreement with observations. This was only a beginning but illustrates the process that is still used.

Mechanical Unfolding of Titin and Fibronectin

A key mechanical function of the human body is motion due to its skeletal muscles and the involuntary muscles of its heart and intestines. Well-known molecular components of muscle are the thin and thick filaments made of actin and myosin, proteins involved in muscle contraction; less known is titin, a protein that gives muscle elasticity and mechanical stability (*23*). Titin is made of about 300 domains and a few random coil segments, all of which are arranged like pearls on a string and act like an elastic, accordion-like band.

Titin is encoded by the longest gene in the human genome; one gene serves for all types of muscle by way of posttranscriptional modification. Although titin in regard to its length is an extreme protein, its architecture is typical of cellular proteins with mechanical function: The protein is highly modular, the modules being homologous in sequence and structure and having systematic sequence differences that translate into specific mechanical properties. One seeks to understand the design of each module and how it contributes individually to titin's mechanical properties while at the same time understanding how all modules together contribute to these properties. The multidomain elasticity stems from pairwise angular reorientations of adjacent domains and is referred to as tertiary structure elasticity, whereas the single-domain elasticity stems from an unraveling of secondary structure elements and thus is called secondary structure elasticity. Random coil segments contribute elasticity that is largely entropic, like in rubber.

Titin in muscle, like other mechanical proteins, must endure and elastically respond to a broad range of forces, acting like a spring in response to weak forces and extending several-fold in length without actually rupturing in response to strong forces. The design principles of titin were little understood until recently. Single-molecule force spectroscopy became a key source of information on mechanical functioning, starting with titin's I91 domains (formerly known as I27), one of the first domain to be structurally resolved (*24*) (Fig. 1 A). In a series of elegant experiments, Gaub *et al*., Bustamante *et al*., and Simmons *et al*. (*25*–*27*) stretched titin by using AFM and optical tweezers. In subsequent work, Fernandez *et al*. stretched engineered tandem domains of I91s in series and monitored the extension-force curve between a substrate and an AFM tip (*28*). In the resulting saw-tooth curves (similar to those shown in Fig. 1, C and E), each tooth represents the stretching and sudden unfolding of one of the domains according to its secondary structure elasticity function. Yet, the information the curves convey, breakpoint extensions and breakpoint forces, is rather limited.

The titin I91 AFM measurements called for an interpretation in terms of the domain's structure, a β-sheet sandwich, as shown in Fig. 1A. The key question was what feature of the structure constitutes the force-bearing part that protects the domain from beginning to unravel apparently without further resistance. SMD simulations offered an opportunity to obtain an answer that could then be tested.

The first SMD simulations (*8*) revealed the force-bearing parts of titin's I91 domain, namely

Department of Physics, University of Illinois at Urbana-Champaign, and Beckman Institute for Advanced Science and Technology, 405 North Mathews Avenue, Urbana, IL 61801, USA.

*To whom correspondence should be addressed. E-mail: kschulte@ks.uiuc.edu

a set of nine interstrand hydrogen bonds between strands A′ and G and between strands A and B (Fig. 1A). The terminal strands A and G are subject to tension when the domain termini are being pulled apart. First, strand A detaches from strand B, leading to an intermediate conformation (Fig. 1B). Then, strand G detaches from strand A′, and, once all nine hydrogen bonds are broken, the remaining strands unravel by unzipping hydrogen bonds one by one. The reverse of the unraveling process most likely is not the route for spontaneous refolding, which rather involves a hydrophobic folding nucleus that is also important for temperature- and denaturant-induced unfolding (*29*–*31*). The force-induced unraveling immediately suggests mutants that should affect the extension-force relation observed in AFM experiments. A key mutant was investigated in a collaboration between Fernandez, Schulten, and co-workers. The mutant, designed to take advantage of the fact that the A-B interstrand hydrogen bonds break a bit more easily than the A′-G bonds do, destabilized further the intermediate and abolished an experimental signature ("hump") in the extension-force curve, corroborating the scenario depicted by simulations (*28*) (Fig. 1C).

Like physical experiments, computational experiments can yield puzzling results. In the case of I91, the height of the energy barrier to stretching the large set of interstrand hydrogen bonds was not well understood (*32*). However, modelers had overlooked a key player, water (*9*). Water molecules continuously attack I91's surface-exposed interstrand hydrogen bonds; one is cut every 10 ps but quickly reforms. This random weakening of hydrogen bonding lowers the force needed to stretch I91 apart and is likely controlled by properties of side groups surrounding them, as is the case for fibronectin (see below) (*33*). Other factors, such as packing interactions, may also influence the mechanical stability of this domain (*31*).

Titin's function likely goes beyond being the passive element of muscle elasticity, acting also as a biomechanical sensor. SMD simulations have suggested that tension can induce exposure of a kinase active site in titin (*34*), thereby transforming mechanical force into a biochemical signal. Similarly, buried binding sites may get exposed when molecules are subject to force, as postulated for other modular proteins (*7*).

Multidomain proteins, made of subunits similar to the ones in titin, act in the extracellular matrix of cells in higher organisms. These proteins, fibronectins, form fibrils that anchor themselves to cell surface receptors, such as integrins, and hold tissue cells together. The fibrils can stretch out to several times their contracted length, giving tissues flexibility. The structures of individual domains and of several tandem domains have been resolved, and their mechanical properties have been investigated by AFM experiments and SMD simulations, showing excellent agreement between the measured and the predicted hierarchy of mechanical stability (*33*, *35*–*37*). Moreover, prediction of intermediate unfolding states has been confirmed by experiments (*38*–*40*). An observed saw-tooth pattern is shown in the Fig. 1E inset. A double peak arises at the tooth that is due to fibronectin domain $FnIII_1$ (*35*), posing a puzzle that was resolved by simulations (*11*).

$FnIII_1$ (Fig. 1 E), like titin I91, has a sandwich architecture of two sheets of β strands but, in contrast to other fibronectin domains, features a small and a large sheet, the size being characterized by substantially different numbers of interstrand hydrogen bonds. This suggested that the main force-bearing hydrogen bonds, i.e., the ones sealing the two β sheets shut, are broken first and the small sheet unravels quickly, but then the large sheet resists further unraveling by aligning itself to the external forces such that a second set of multiple interstrand hydrogen bonds needs to be ruptured before the remainder of the sheet unzips. This pathway depends on detailed structural features that were unknown because of the lack of a resolved structure. Homology modeling based on the known structures of other fibronectin domains proved that the proposal could explain the intermediate states observed in AFM experiments (Fig. 1E). Our collaboration with Campbell led to the structure of $FnIII_1$ being solved by nuclear magnetic resonance (NMR) spectroscopy. This structure further corroborated the model, revealing key details that strengthen the large $FnIII_1$ sheet (*11*).

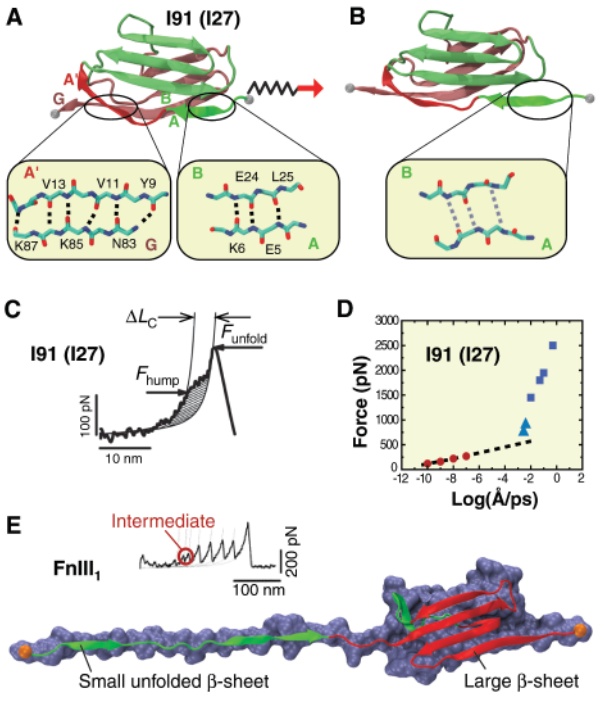

Fig. 1. Titin I91 and $FnIII_1$ elasticity. (**A**) Titin I91 (formerly known as I27) is shown in cartoon representation. The two β sheets forming the domain are shown in green and red. Detail of backbone hydrogen bonds involving β strands A-B and A′-G are shown. E, Glu; K, Lys; L, Leu; N, Asn; V, Val; and Y, Tyr. (**B**) Stretching of titin I91 through SMD simulation reveals an intermediate state in which β strand A is detached from β strand B, yet β strands A′ and G are still connected. (**C**) Force peak corresponding to unfolding of one titin domain obtained through AFM experiments [adapted from (*28*)]. The unusual "hump" observed in the force peak arises due to the unfolding intermediate [(B)] identified by SMD simulations (*70*). A point mutation disrupting backbone hydrogen bonds that link β strands A and B removed the observed hump. (**D**) Dependence on stretching velocity (in units of Å/ps) of the rupture force peak of titin I91. Red circles represent values from AFM experiments; blue squares and triangles represent values from constant velocity and constant force SMD simulations, respectively [adapted from (*10*); see also (*71*)]. The SMD data approaches the extrapolated AFM force peak curve upon reduction of velocity, as expected. (**E**) Intermediate state of $FnIII_1$ obtained through SMD simulations (shown in cartoon and surface representations). The small, unfolded β sheet is shown in green. (Inset) A "saw-tooth" pattern for $FnIII_1$, revealing the existence of intermediate states [adapted from (*35*)]. This intermediate state is thought to be relevant in the formation and strengthening of fibronectin fibrils.

What is the purpose of the peculiar architecture of $FnIII_1$? It was suggested that the large $FnIII_1$ sheet offers interstrand binding opportunities to domains of parallel fibers, leading to cross-linking in a sufficiently stretched extracellular matrix (*11*). Amazingly, the large sheet of $FnIII_1$ is an anticancer drug, anastellin, that apparently prevents metastasis by strengthening the adhesion of cancer cells to primary tissue cells (*11*, *41*).

Linker-Mediated Elasticity of Spectrin

The discoidal shape and mechanical properties of red blood cells assist their rapid adaptation to wide arteries and narrow capillaries. Diseases, such as hereditary spherocytosis and elliptocytosis, causing hemolytic anemia are associated with a lack of an elastic, adaptable shape caused by mutations affecting the red blood cell cytoskeletal network made of spectrin, ankyrin, and associated proteins (*42*–*44*).

The elastic architecture of the protein modules forming titin and fibronectin described above differs from that of spectrin repeats found in the red blood cell cytoskeleton. Crystal structures

of the superfamily of spectrin proteins, including spectrin itself, α-actinin, and dystrophin, reveal building blocks made of three-helix bundles repeated in series (Fig. 2) and forming part of heterotetrameric assemblies arranged in elongated filaments (*42*, *45*). The structures also revealed an α-helical linker. However, the static structures cannot reveal elastic properties, and therefore researchers turned to AFM experiments and SMD simulations to investigate spectrin elasticity.

Initial AFM experiments (*46*) suggested that spectrin repeats mechanically unfold predominantly one by one in an independent, all-or-none fashion. Force peaks were found to be substantially smaller than those observed for other proteins made of β strands instead of α helices. Further AFM experiments confirmed the relative weakness of spectrin and the one-by-one unfolding pathway but also revealed that different sets of spectrin repeats may exhibit intermediates and cooperative unfolding events involving more than one repeat (*47*–*49*) (bottom trace in Fig. 2 inset). Forces and distances obtained from AFM characterized well the elasticity of spectrin, but the molecular mechanism underlying spectrin elasticity could only be identified through simulation.

SMD simulations of two or more spectrin repeats solvated in explicit water (*12*, *13*) confirmed the relative weakness of spectrin when compared with the immunoglobulin-like domains of titin and fibronectin. The simulations also confirmed the existence of different unfolding pathways and suggested that the spectrin elastic response is rate dependent (*12*). Despite the large stretching velocities used in the simulations (*50*), the results matched qualitatively the prior experimental characterization. Moreover, simulations identified the linker regions between spectrin repeats as key elastic elements (*12*, *13*). Analysis of simulated unfolding, which followed the motion of all the atoms of the protein-solvent system during stretching, permitted researchers to identify which regions unfold first (the linker regions), the key amino acids involved in rupture of secondary and tertiary structure elements, and the role of water during unfolding (Fig. 2).

The detailed unfolding pathway gleaned from SMD simulations complement the AFM experiments. However, can the simulations also be predictive? Indeed they can. Recent work identified mutations at the linker regions of spectrin causing disease (*44*), thereby corroborating the relevance of linkers in the mechanical response of this protein as indicated by simulations. The mutations, involving substitution of amino acids by proline, destabilize the α-helical structure of the linker and favor temperature-mediated unfolding of spectrin as probed through in vitro experiments (*44*).

Ankyrin Elasticity

The third protein system reviewed here, ankyrin, is an example of simulation being ahead of experiments. Ankyrin proteins were first identified as essential components of the red blood cell cytoskeleton, providing a link between spectrin and membrane-bound ion channels (*42*). Although the specific role of ankyrins was unknown, their sequence revealed a repetitive motif of 33 amino acids named the ankyrin repeat. This motif is found in sets of 24 throughout the family of ankyrins. Such ankyrin repeats were later found to be part of the sequence of hundreds of other proteins (*51*) and are now widely recognized as ubiquitous molecular components of living cells. Ankyrin repeats are thought to mediate protein-protein interactions (*52*), but otherwise their function remains unclear.

The three-dimensional structure of the ankyrin repeat motif is well conserved (*52*–*54*). Each repeat is made of two antiparallel α helices and a short loop. Repeats stack in parallel, sharing a large hydrophobic interface and featuring another, slightly larger, connecting loop (Fig. 3A). The parallel arrangement of ankyrin repeats contrasts the arrangement of the modular proteins described above. Titin, fibronectin, and spectrin feature modules arranged linearly in series, whereas the ankyrin parallel arrangement results in elongated proteins featuring a superhelical conformation when multiple repeats are put together (Fig. 3B). Moreover, amino acids that are close in sequence are also close in space. An interest in ankyrin repeats came from the finding that transient receptor potential channels, thought to mediate mechanotransduction in higher organisms, contain up to 29 ankyrin repeats that might gate such channels (*55*, *56*). Both experimental and computational groups sought to characterize the elasticity of ankyrin.

SMD simulations performed on multiple crystal structures and models of ankyrin repeats were the first to examine the elastic properties of these repeat proteins (*14*). Simulations performed on structures containing 4, 12, and 24 ankyrin repeats revealed a two-stage elastic response. On application of force, the protein first changes its shape from helical to straight by rearranging tertiary structure elements but keeping the secondary structure intact (Fig. 3B). Then, on increasing force, repeats detach and unfold from the structure. The initial curved-to-straight transition is reversible, and, indeed, large stacks of ankyrin repeats behave like an overdamped spring. The response corresponds to tertiary structure elasticity.

After the initial elongation, simulations revealed a saw-tooth pattern depicting detachment and unfolding of individual repeats, one at a time (Fig. 3C), corresponding to secondary structure elasticity. Constant-force SMD simulations found stepwise unfolding of ankyrin repeats characterized by steps of ~100 Å (*14*).

AFM experiments by Marszalek *et al*. and Fernandez *et al*. confirmed the simulation results (*57*, *58*). Experiments performed on 24 ankyrin repeats of human ankyrin-B showed a Hookean response at low force that closely matched (within a factor of two) the linear elastic response observed in simulations of human ankyrin-R attributed to tertiary structure elasticity (*57*) (Fig. 3D). Experiments also revealed the stepwise unfolding of individual repeats separated by distances of 11 nm (*57*, *58*) (Fig. 3D, inset). Although the forces observed for unfolding of individual ankyrin domains in vitro are substantially lower than those observed in silico [as expected because of the high stretching velocity used in simulations (*50*)], the hierarchy of mechanical stability and the observed peak-to-peak distances determined using both methods are consistent (*59*).

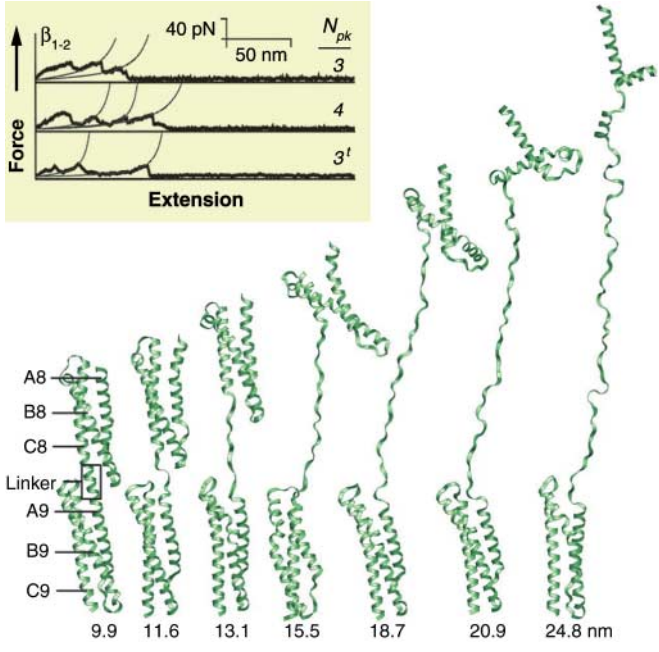

Fig. 2. Elasticity of spectrin. Mechanical unfolding of a double-repeat β-spectrin from human erythrocytes [adapted from (*13*)]. Each spectrin repeat (labeled 8 and 9) is made of three α helices denoted as A, B, and C. The unfolding sequence shows how the linker region unfolds first. (**Inset**) Force-extension curves for a two-β-spectrin repeat construct [adapted from (*48*)]. The bottom trace shows cooperative unfolding. Mutations weakening the linker region of spectrin have been shown to cause hereditary spherocytosis (*44*).

Outlook

The examples described highlight the role of modeling in the quest to

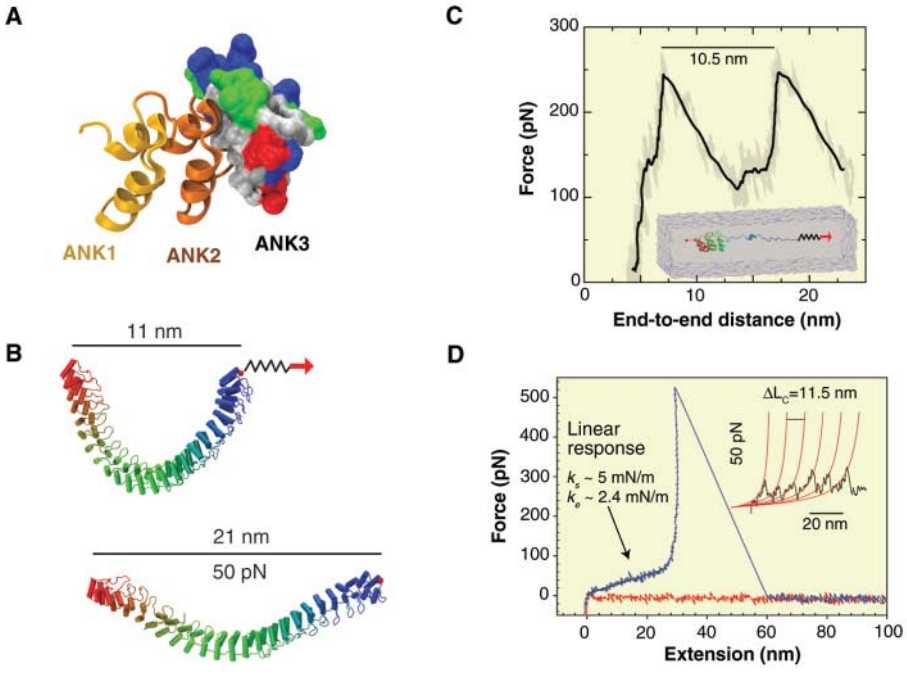

Fig. 3. Elasticity of repeat proteins. (**A**) Architecture of three ankyrin repeats (two shown in yellow and orange cartoon, and one shown in surface representation with colors indicating residue type). (**B**) Equilibrated conformation of human ankyrin-R (24 repeats) and a stretched state obtained after 6 ns of SMD simulation using a constant force of 50 pN (k_s ~ 5 mN/m). Molecules are shown in cartoon representation and colored from red (repeat 1) to blue (repeat 24). (**C**) The simulated force-extension profile of ankyrin unfolding exhibits two force peaks separated by 10.5 nm, corresponding to unraveling and unfolding of individual repeats (secondary structure elasticity). (Inset) The hydrated system simulated. (**D**) The experimental force-extension profile obtained upon stretching of 24 ankyrin repeats of human ankyrin-B is shown in blue [adapted from (*57*)]. The linear response ($\langle k_e \rangle$ ~ 2 mN/m) observed in AFM experiments corresponds well to predicted tertiary structure elasticity (k_s ~ 5 mN/m) observed in SMD simulations of 24 ankyrin repeats (*14*). (Inset) The force-extension profile of six ankyrin repeats obtained through AFM experiments [adapted from (*58*)] features six peaks separated by 11.5 ± 0.7 nm, in close agreement with predicted secondary structure elasticity. The magnitude of the forces are about one order of magnitude smaller than those observed in SMD simulations, as expected from the dependence of force peak values on the stretching velocity (*50*).

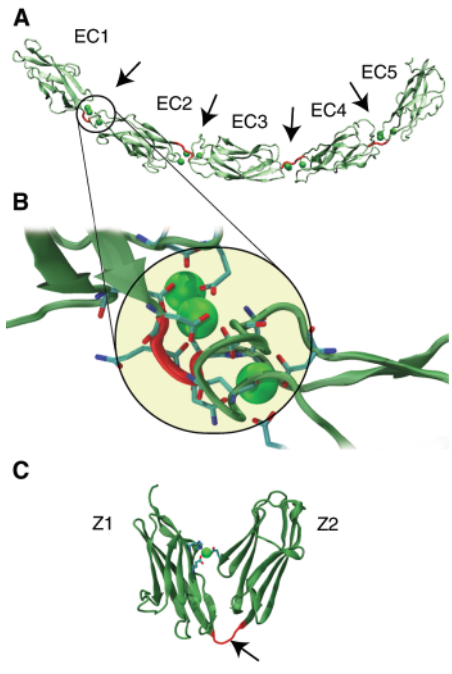

Fig. 4. Linker-mediated elasticity of modular proteins. (**A**) Crystal structure of the complete C-cadherin extracellular domain, featuring five modules labeled EC1 to EC5 (*61*). The protein is shown in cartoon representation. Arrows point at linker regions depicted in red. Calcium ions binding at the linker regions are shown as green spheres. (**B**) Detail of C-cadherin EC1-EC2 linker. Interactions of calcium ions with charged amino acids at the linker region determine the elastic behavior of the protein and its adhesive properties. (**C**) Crystal structure of titin Z1Z2 modules (*65*) shown in cartoon representation. The structure depicts a closed-hinge conformation induced by binding of a metal ion and flexibility of the linker region (arrow) depicted in red.

determine the mechanical properties of proteins that are subject to force in vivo. Although in vitro experiments in which force is applied to biomolecules opened a completely new field of research, in silico experiments, despite their limitations (*50*, *59*), have resolved the molecular mechanisms underlying the elastic response of biomolecules. Identification of the force-bearing regions of titin, the role of hydrogen bonds and water during mechanical unfolding of immunoglobulin-like domains, the intermediate states of fibronectin, the role of linkers in spectrin mechanics, and the tertiary structure elasticity of ankyrin repeats were only possible through simulations combined with experiments.

Simulations are now going beyond single domain proteins as crystal structures of larger protein complexes become available and computing power increases. Such simulations seek to characterize the important role of linkers in the elasticity of proteins containing many globular domains. Cadherins (*5*, *60*, *61*), for instance, mediate calcium-dependent cell-cell adhesion. SMD simulations of a single cadherin domain (*14*) had already shown the relevance of linkers and calcium ions on its elastic response. Equilibrium (*62*) and SMD simulations of proteins containing multiple cadherin domains have now revealed the flexibility and tertiary structure elasticity of these modular proteins (Fig. 4A). SMD simulations have shown how tertiary and secondary structure elasticity of the complete cadherin domain is controlled through calcium ions bound to linker regions (Fig. 4B), a property that is not only relevant for cell-cell adhesion but also important in hearing (*56*, *14*) where cadherin-23 forms part of the mechanotransduction apparatus (*63*, *64*).

A recent structure of Z1-Z2 domains of titin (*65*) (Fig. 4C) indicates that linkers may play a role in titin elasticity as well. Depending on the length and structure of the linker, different titin modules may exhibit a varied repertoire of elastic responses. Even more suggestive is the fact that a divalent ion outside of the linker region induces a "closed-hinge" conformation in the crystal structure; similar binding sites were predicted through modeling for titin I91 (*8*).

Ultimately, understanding the molecular mechanisms involved in the force response of proteins should lead to the design of structures with desired elastic properties, and surely modeling will play an important role in such endeavor.

References and Notes

1. Molecular dynamics (MD) simulations have their bases in theoretical models describing interactions between atoms through so-called force fields (*66*–*68*). In a typical MD simulation, initial coordinates of the atoms in a macromolecule are obtained from crystallographic or NMR structures. The structure is then solvated in water, and the motion of atoms in time is determined through integration of Newton's equations (*68*) assuming the mentioned force field. Current simulation packages, such as NAMD (*68*), use standardized force fields and provide the source code of the simulation engine. The widespread use and availability of the software and force fields ensures constant verification and reproducibility of results.
2. SMD simulations apply, in addition to indigenous forces, external forces to biomolecules (*17*). There are two typical protocols for SMD simulations: constant force and constant velocity. In constant force SMD simulations, a force is directly applied to one or more atoms, and extension or displacement is monitored throughout dynamics. Customized time-dependent forces may be applied as well. In constant velocity

SMD simulations, a moving harmonic potential (spring) is used to induce motion along a reaction coordinate. The free end of the spring is moved at constant velocity, while the protein atoms attached to the other end of the spring are subject to the steering force. The force applied is determined by the extension of the spring and can be monitored throughout the entire simulation.
3. A. D. Mehta, M. Rief, J. A. Spudich, D. A. Smith, R. M. Simmons, *Science* **283**, 1689 (1999).
4. J. Zlatanova, K. van Holde, *Mol. Cell* **24**, 317 (2006).
5. D. Leckband, A. Prakasam, *Annu. Rev. Biomed. Eng.* **8**, 259 (2006).
6. M. Gao, M. Sotomayor, E. Villa, E. Lee, K. Schulten, *Phys. Chem. Chem. Phys.* **8**, 3692 (2006).
7. V. Vogel, *Annu. Rev. Biophys. Biomol. Struct.* **35**, 459 (2006).
8. H. Lu, B. Isralewitz, A. Krammer, V. Vogel, K. Schulten, *Biophys. J.* **75**, 662 (1998).
9. H. Lu, K. Schulten, *Biophys. J.* **79**, 51 (2000).
10. M. Gao, H. Lu, K. Schulten, *J. Muscle Res. Cell Motil.* **23**, 513 (2002).
11. M. Gao *et al.*, *Proc. Natl. Acad. Sci. U.S.A.* **100**, 14784 (2003).
12. V. Ortiz, S. O. Nielsen, M. L. Klein, D. E. Discher, *J. Mol. Biol.* **349**, 638 (2005).
13. S. Paramore, G. A. Voth, *Biophys. J.* **91**, 3436 (2006).
14. M. Sotomayor, D. P. Corey, K. Schulten, *Structure* **13**, 669 (2005).
15. Z. Lu, H. Hu, W. Yang, P. E. Marszalek, *Biophys. J.* **91**, L57 (2006).
16. M. Carrion-Vazquez *et al.*, *Nat. Struct. Biol.* **10**, 738 (2003).
17. B. Isralewitz, M. Gao, K. Schulten, *Curr. Opin. Struct. Biol.* **11**, 224 (2001).
18. H. Grubmüller, *Methods Mol. Biol.* **305**, 493 (2005).
19. E.-L. Florin, V. T. Moy, H. E. Gaub, *Science* **264**, 415 (1994).
20. H. Grubmüller, B. Heymann, P. Tavan, *Science* **271**, 997 (1996).
21. S. Izrailev, S. Stepaniants, M. Balsera, Y. Oono, K. Schulten, *Biophys. J.* **72**, 1568 (1997).
22. E. Evans, K. Ritchie, *Biophys. J.* **72**, 1541 (1997).
23. L. Tskhovrebova, J. Trinick, *Nat. Rev. Mol. Cell Biol.* **4**, 679 (2003).
24. S. Improta, A. Politou, A. Pastore, *Structure* **4**, 323 (1996).
25. M. Rief, M. Gautel, F. Oesterhelt, J. M. Fernandez, H. E. Gaub, *Science* **276**, 1109 (1997).
26. M. S. Z. Kellermayer, S. Smith, H. Granzier, C. Bustamante, *Science* **276**, 1112 (1997).
27. L. Tskhovrebova, J. Trinick, J. Sleep, R. Simmons, *Nature* **387**, 308 (1997).
28. P. E. Marszalek *et al.*, *Nature* **402**, 100 (1999).
29. S. B. Fowler *et al.*, *J. Mol. Biol.* **322**, 841 (2002).
30. P. M. Williams *et al.*, *Nature* **422**, 446 (2003).
31. R. B. Best *et al.*, *J. Mol. Biol.* **330**, 867 (2003).
32. H. Lu, K. Schulten, *Proteins Struct. Funct. Genet.* **35**, 453 (1999).
33. D. Craig, M. Gao, K. Schulten, V. Vogel, *Structure* **12**, 21 (2004).
34. F. Gräter, J. Shen, H. Jiang, M. Gautel, H. Grubmüller, *Biophys. J.* **88**, 790 (2005).
35. A. F. Oberhauser, C. Badilla-Fernandez, M. Carrion-Vazquez, J. Fernandez, *J. Mol. Biol.* **319**, 433 (2002).
36. D. Craig, A. Krammer, K. Schulten, V. Vogel, *Proc. Natl. Acad. Sci. U.S.A.* **98**, 5590 (2001).
37. R. W. S. Rounsevell, J. Clarke, *Structure* **12**, 4 (2004).
38. E. Paci, M. Karplus, *J. Mol. Biol.* **288**, 441 (1999).
39. M. Gao, D. Craig, V. Vogel, K. Schulten, *J. Mol. Biol.* **323**, 939 (2002).
40. L. Li, H. H. Huang, C. L. Badilla, J. M. Fernandez, *J. Mol. Biol.* **345**, 817 (2005).
41. M. Yi, E. Ruoslahti, *Proc. Natl. Acad. Sci. U.S.A.* **98**, 620 (2001).
42. V. Bennett, A. J. Baines, *Physiol. Rev.* **81**, 1353 (2001).
43. D. E. Discher, P. Carl, *Cell. Mol. Biol. Lett.* **6**, 593 (2001).
44. C. P. Johnson *et al.*, *Blood* **109**, 3538 (2007).
45. H. Kusunoki, R. I. MacDonald, A. Mondragón, *Structure* **12**, 645 (2004).
46. M. Rief, J. Pascual, M. Saraste, H. Gaub, *J. Mol. Biol.* **286**, 553 (1999).
47. S. M. Altmann *et al.*, *Structure* **10**, 1085 (2002).
48. R. Law *et al.*, *Biophys. J.* **84**, 533 (2003).
49. L. G. Randles, R. W. S. Rounsevell, J. Clarke, *Biophys. J.* **92**, 571 (2007).
50. The magnitude and fluctuations of the monitored forces in constant-velocity SMD simulations will depend on the stretching velocity and spring constant used (*21*, *22*). The smaller the velocity used, the less drastic the perturbation of the system is, and more details along the reaction coordinate are likely to be captured. Because of limitations in computational resources, even the slowest stretching velocities used in simulations are orders of magnitude faster than those used in equivalent AFM stretching experiments. The force peak values observed will then be larger than those recorded in experiments (Fig. 1D). The dependence of the monitored force on the stretching velocity is more relevant for secondary structure elasticity than for tertiary structure elasticity, because in the latter case solvent effects due to friction and hydrogen bond attack play a less important role.
51. P. J. Mohler, A. O. Gramolini, V. Bennett, *J. Cell Sci.* **115**, 1565 (2002).
52. L. K. Mosavi, T. J. Cammett, D. C. Desrosiers, Z. Peng, *Protein Sci.* **13**, 1435 (2004).
53. L. K. Mosavi, D. L. Minor, Z. Peng, *Proc. Natl. Acad. Sci. U.S.A.* **99**, 16029 (2002).
54. P. Michaely, D. R. Tomchick, M. Machius, R. G. W. Anderson, *EMBO J.* **21**, 6387 (2002).
55. J. Howard, S. Bechstedt, *Curr. Biol.* **14**, R224 (2004).
56. D. P. Corey, M. Sotomayor, *Nature* **428**, 901 (2004).
57. G. Lee *et al.*, *Nature* **440**, 246 (2006).
58. L. Li, S. Wetzel, A. Pluckthun, J. M. Fernandez, *Biophys. J.* **90**, L30 (2006).
59. It is often noticed that SMD simulations yield "wrong" unfolding force values when compared with AFM measurements. Such a statement is obviously illogical, because SMD simulations must yield stronger forces because of the faster pulling velocity. Faster pulling may alter the nature of the protein's elastic response, but AFM extensions can be directly compared with SMD extensions, offering a test of the concern.
60. M. Takeichi, *Annu. Rev. Biochem.* **59**, 237 (1990).
61. T. J. Boggon *et al.*, *Science* **296**, 1308 (2002); published online 18 April 2002 (10.1126/science.1071559).
62. F. Cailliez, R. Lavery, *Biophys. J.* **89**, 3895 (2005).
63. C. Söllner *et al.*, *Nature* **428**, 955 (2004).
64. J. Siemens *et al.*, *Nature* **428**, 950 (2004).
65. M. Marino *et al.*, *Structure* **14**, 1437 (2006).
66. A. MacKerell Jr. *et al.*, *J. Phys. Chem. B* **102**, 3586 (1998).
67. S. A. Adcock, J. A. McCammon, *Chem. Rev.* **106**, 1589 (2006).
68. J. C. Phillips *et al.*, *J. Comput. Chem.* **26**, 1781 (2005).
69. W. Humphrey, A. Dalke, K. Schulten, *J. Mol. Graph.* **14**, 33 (1996).
70. H. Lu, K. Schulten, *Chem. Phys.* **247**, 141 (1999).
71. M. Rief, H. Grubmüller, *ChemPhysChem* **3**, 255 (2002).
72. The work reviewed here involved many researchers from our own and other groups. We apologize to all researchers whose pioneering work could not be reviewed because of space limitation. We thank M. Gao, B. Isralewitz, S. Izrailev, H. Lu, J. C. Gumbart, and members of the Theoretical and Computational Biophysics Group for their contributions and helpful discussions; our long-time collaborator, V. Vogel, for guidance and inspirations; collaborators D. P. Corey, D. Craig, A. Krammer, O. Mayans, and M. Wilmanns; and J. Fernandez and P. Marszalek for a wonderful experimental-theoretical collaboration. The molecular images in this paper were created with the molecular graphics program VMD (*69*) and Tachyon. This work was supported by funds of the NIH (grant no. P41 RR05969 and grant no. 1 R01 GM073655) and the Humboldt Foundation (K.S.). The authors also acknowledge computer time provided by the NSF through the Large Resource Allocations Committee grant MCA93S028.

10.1126/science.1137591

REVIEW

Forces and Bond Dynamics in Cell Adhesion

Evan A. Evans[1,2]* and David A. Calderwood[3]

Adhesion of a biological cell to another cell or the extracellular matrix involves complex couplings between cell biochemistry, structural mechanics, and surface bonding. The interactions are dynamic and act through association and dissociation of bonds between very large molecules at rates that change considerably under stress. Combining molecular cell biology with single-molecule force spectroscopy provides a powerful tool for exploring the complexity of cell adhesion, that is, how cell signaling processes strengthen adhesion bonds and how forces applied to cell-surface bonds act on intracellular sites to catalyze chemical processes or switch molecular interactions on and off. Probing adhesion receptors on strategically engineered cells with force during functional stimulation can reveal key nodes of communication between the mechanical and chemical circuitry of a cell.

The physical role of a cell adhesion bond is to hold a cell to other cells or to tissue substrata while supporting the forces involved in cell function. Complicating this task, a single adhesion bond effectively resists force only for time periods less than that needed for its spontaneous dissociation under thermal activation. Thus, the diversity in the mechanochemistry of adhesion bonds reflects how mechanical force applied to a bond between a pair of interacting molecules alters activation energy barriers along kinetic pathways, or switches pathways, that lead to dissociation. Viewed ideally as illustrated by Fig. 1, applying adhesion stress through the local material structure to a bond is conceptually like pulling on the chemical interaction with a mechanical spring that mimics the compliance properties of structures attached to the binding site. Stretching this equivalent spring produces a force that lowers the chemical activation barrier to increase the frequency of bond dissociation while, at the same time, the spring potential defines an "energy well" that captures the dissociated states and regulates the likelihood of rebinding. Focusing our discussion on adhesive interactions in soft tissues and organs of